HHS Public Access

Author manuscript

Biol Psychiatry. Author manuscript; available in PMC 2019 March 15.

Published in final edited form as:

Biol Psychiatry. 2018 March 15; 83(6): 499–508. doi:10.1016/j.biopsych.2017.10.024.

A schizophrenia-linked *KALRN* coding variant alters neuron morphology, protein function, and transcript stability

Theron A. Russell, MS[*,1], **Melanie J. Grubisha, MD, PhD**[*,2,3], **Christine L. Remmers, BS**[1], **Seok Kyu Kang, BS**[1], **Marc P. Forrest, PhD**[1], **Katharine R. Smith, PhD**[1], **Katherine J. Kopeikina, PhD**[1], **Ruoqi Gao, BS**[1], **Robert A. Sweet, MD**[2,3,4], and **Peter Penzes, PhD**[1,5]

[1]Department of Physiology, Northwestern University Feinberg School of Medicine, Chicago, IL

[2]Department of Psychiatry, University of Pittsburgh School of Medicine, Pittsburgh, PA

[3]Department of Neurology, University of Pittsburgh School of Medicine, Pittsburgh, PA

[4]VISN 4 Mental Illness Research, Education and Clinical Center (MIRECC), VA Pittsburgh Healthcare System, Pittsburgh, PA

[5]Department of Psychiatry and Behavioral Sciences, Northwestern University Feinberg School of Medicine, Chicago, IL

Abstract

Background—Large-scale genetic studies have revealed that rare sequence variants, including single nucleotide variants (SNVs), in glutamatergic synaptic genes are enriched in schizophrenia (SZ) patients. However, the majority are too rare to show any association with disease, and have not been examined functionally. One such SNV, *KALRN*-P2255T displays a penetrance which greatly exceeds that of previously identified SZ-associated SNVs. Therefore, we sought to characterize its effects on the function of Kalirin-9 (Kal9), a dual Rac1 and RhoA guanine nucleotide exchange factor (GEF), upregulated in human SZ brain tissue.

Methods—Kal9 was overexpressed in primary rat cortical neurons or hEK293 cells. The effects of the P2255T variant on dendritic branching, dendritic spine morphology, protein and mRNA stability, and catalytic activity were examined.

Results—Kal9-P2255T leads to diminished basal dendritic branching and dendritic spine size, compared to wildtype Kal9 (Kal9-WT). The P2255T SNV directly affected Kal9 protein function, causing increased RhoA activation in hEK203 cells, but had no effect on Rac1 activation. Consistent with human postmortem findings, we found that Kal9-P2255T protein levels were higher than those of Kal9-WT in neurons. Increased mRNA stability was detected in hEK293

Corresponding author: Peter Penzes, Ward Bldg., Rm. 5-654, 303 E. Chicago Ave., Chicago, IL 60611, Phone: 312-503-5379, Fax: 312-503-5101, p-penzes@northwestern.edu.

*contributed equally

Conflicts of interest

The authors report no biomedical financial interests or potential conflicts of interest.

cells, indicating that this was the cause of the higher protein levels. When analyzed together, increased intrinsic RhoA-GEF catalytic activity combined with increased mRNA expression led to net enhancement of RhoA activation, known to negatively impact neuronal morphology.

Conclusions—Taken together, our data reveal a novel mechanism for disease-associated SNVs and provide a platform for modeling morphological changes in mental disorders.

Keywords

Dendrites; Dendritic spines; Guanine nucleotide exchange factors; Kalirin; Schizophrenia; Single nucleotide variants

Introduction

Schizophrenia (SZ) is a debilitating and highly heritable psychiatric disorder characterized by alterations in perception, affect, and cognition. Although heritability of SZ has been estimated at 80%, its genetic architecture is highly complex, including common variants with very small effects and relatively rare copy number variants with large effect sizes (1, 2). In addition to these, large-scale exome sequencing studies revealed that exonic point mutations (single nucleotide variants or SNVs), play an important role in the etiology of mental disorders, including SZ (3–5). These SNVs are overrepresented among glutamatergic postsynaptic proteins that modulate the cytoskeleton. Such variants are very rare (frequency < 0.5%), precluding statistical association. Understanding the functional significance of such mutations, especially at sites relevant for these disorders such as dendrites, would provide insight into the biological functions of rare SNVs in the pathogenesis of SZ. Focusing on SNVs with any statistical association with SZ would strengthen the overall relevance.

Previously, a SZ-associated non-synonymous SNV in the human *KALRN* gene (rs143835330), that codes for a proline to threonine substitution was identified and subsequently confirmed in multiple cohorts (6). The allele frequency of the P2255T variant was shown to be 0.011 in SZ patients as compared to 0.005 in controls. This variant has an OR>2, a higher effect size than any previously reported for other SZ-associated nonsynonymous coding variants (7). Notably, postmortem studies found kalirin mRNA and levels of the kalirin-7 (Kal7) protein isoform to be reduced in the prefrontal cortex (8, 9), while kalirin-9 (Kal9) was increased in the auditory cortex in subjects with SZ (10), suggesting a role for kalirin in SZ pathophysiology.

Alternate splicing of *KALRN* gives rise to several protein isoforms, the major ones being Kalirin-7, -9, and -12 (11). Of these, the P2255 residue is only present in the longer Kalirin-9 and -12 isoforms. These proteins include several protein-protein interaction domains, along with a Rac1 and a RhoA guanine nucleotide exchange factor (GEF) domain (Figure 1A) (12). RhoA and Rac1 are “molecular switches” with established roles in dendrite and dendritic spine morphogenesis (13, 14). When activated, GTPases can bind various effector proteins, which in turn induce cytoskeletal changes. In general, Rac1 promotes dendrite arborization and spine growth and stabilization, while RhoA inhibits these processes (15–17). Recently, the spatial and temporal regulation of these GTPases' oscillations between active and inactive states was shown to coordinate distinct forms of

excitatory synaptic plasticity (18). Furthermore, overexpression of the Rho-GEF ARHGEF11 or constitutively active RhoA, as well as the knockdown of the Rho GTPase activating protein oligophrenin-1, have been shown to reduce dendritic complexity, spine area, and spine density (19–21).

Kalirin has also been implicated in several signaling pathways previously shown to be relevant for SZ. The Kal7 isoform localizes to the synapse where it interacts with DISC1 and regulates spine formation through Rac1 (22). Kal7 is also regulated via phosphorylation downstream of neuregulin-1 and ErbB receptors (23). PAK family members, which act downstream of kalirin and Rac1, are dysregulated in SZ and other psychiatric disorders (9, 24, 25). Finally, analysis of the network of kalirin-related gene products demonstrates a significant overlap between the kalirin network and genes that have been linked to SZ via GWAS (Figure 1B, C; Supplemental Figure S1) (26, 27). These observations suggest that kalirin is involved in a network of synaptic proteins that are crucial for synaptic function, and whose disruptions likely contribute to SZ pathology.

Because spine loss and reduction in dendritic arbor size has been reproducibly reported in multiple brain regions including the dorsolateral prefrontal cortex and primary auditory cortex in SZ patients (28, 29), we aimed to investigate the functional impact of the *KALRN*-P2255T SNV on dendritic morphology. We have previously shown that Kal9 levels are increased in the auditory cortex of SZ patients, and that its overexpression in cortical neurons causes diminished dendritic branching and altered dendritic spine morphologies that are reminiscent of morphological abnormalities observed in postmortem tissue from schizophrenia patients (10). We thus investigated the role of the P2255T variant expressed in the Kal9 isoform background. Structured illumination microscopy revealed differential subsynaptic distribution of kalirin isoforms. We found that overexpression of the P2255T variant led to morphological changes in cultured neurons that are consistent with those seen in SZ. Additionally, we also observed increased mRNA stability of Kal9-P2255T, leading to increased mRNA expression and protein levels compared to controls. Finally, we determined that the P2255T increased Kal9 Rho-GEF activity, but had no effect on Rac-GEF activity. Thus, the combination of both altered protein function and increased protein levels likely contribute to the pathogenesis of SZ in patients carrying this SNV. This mutation provides an effective model for further investigating convergent pathways underlying perturbed dendritic morphogenesis in SZ.

Methods

(Extended methods are presented in Supplemental Information).

Cell culture, Transfection

High density cortical neuronal cultures were derived from embryonic day 17 (E17) Sprague Dawley rats (Envigo, Indianapolis, IN; and Charles River Laboratories, Worcester, MA). They were cultured as previously described (30, 31). All transfections were performed using Lipofectamine LTX with Plus reagent or Lipofectamine 2000 (ThermoFisher Scientific, Grand Island, NY) in the absence of antibiotics. All procedures involving animals were approved by the Northwestern University Animal Care and Use Committee.

qRT-PCR and Western Blotting

Isoform-specific primers were used to detect Kal9. Real-time quantitative PCR was performed on a Step-One Plus (Applied Biosystems, Foster City, CA) using Sybr Green (Bio-Rad, Hercules, CA). Results were analyzed using the comparative Ct method.

Immunofluorescence, imaging, and image processing

For the analysis of Kal9 protein expression, data acquisition was performed on an Olympus (Center Valley, PA) BX51 WI upright microscope equipped with an Olympus spinning disk confocal. For the analyses of dendritic branching and spine morphology, images were acquired with a Zeiss LSM5 Pascal confocal microscope (Carl Zeiss Microscopy, Thornwood, NY). Dendrites were analyzed using the Fiji Sholl analysis plugin (32). Spine analysis was performed as described previously (33). Multichannel SIM imaging and analysis were performed as described previously (34).

GTPase Activation Assays

Active RhoA and Rac1 levels were evaluated via Western blotting with the RhoA and Rac1 Pull-down Activation Assays (Cytoskeleton, Inc., Denver, CO) as described previously (35).

Statistical Analysis

Comparisons between transcript and protein levels were performed using a two-tailed, unpaired student's t-test. Rates of degradation were calculated using a linear regression. Transcript half-life was determined using $t_{1/2}$= ln(2)/-slope. Effects on spine parameters and GTPase activation were analyzed using a two-tailed unpaired t-test. Sholl analysis data were assessed by two-way ANOVA, followed by Bonferroni correction for multiple comparisons. All data were gathered with the experimenter blinded to condition.

Results

Superresolution imaging reveals differential subsynaptic localization of kalirin isoforms

To establish the subcellular sites where Kal9-P2255T-dependent cellular phenotypes may be more evident, we examined the relative subcellular distribution of major kalirin isoforms. To determine the relative spatial localization of kalirin isoforms in mature neurons, we used structured illumination microscopy (SIM), a superresolution method (36) to determine the precise localization of Kal7 and Kal9 (Figure 1D). Notably, the relative subsynaptic distribution of different isoforms of a postsynaptic protein has not yet been examined at the sub-diffraction level. Whereas Kal7 was present in 75% of spines, Kal9 was predominantly expressed in shafts or excluded entirely, with only 31% of spines that were examined expressing this isoform (Figure 1E). Furthermore, although spines which included Kal7 tended to be significantly larger than those which did not, the presence of Kal9 in spines did not correlate with spine morphology (Figure 1F). These data suggest that spatial patterning of kalirin isoforms may play an important role in dendrite and spine structure, with Kal9 likely exerting its primary effects on cytoskeletal remodeling in dendrites..

Kal9-P2255T reduces basal dendrite branching

To determine the impact of the P2255T SNV on dendritic morphology, we overexpressed Kal9-WT or Kal9-P2255T, along with GFP, in cultured cortical neurons (DIV 25–26) (Figure 2A). As expected (10), overexpression of Kal9-WT led to significant reductions in both basal and apical dendritic complexity as compared to cells transfected with only GFP (Figure 2B). Kal9-P2255T overexpression led to a significant reduction of proximal dendritic complexity as compared to Kal9-WT (Figure 2B, left panel). This overall reduction was due to an approximate 25% reduction in the number of basal dendrites extending 25 and 50 μm from the soma (Figure 2B, right panel). The functional consequences of this reduction are unknown; however, the synapses on proximal versus distal basal dendrites are known to undergo distinct mechanisms of plasticity and have distinct roles in the temporal and spatial summation of excitatory inputs (37, 38).

Kal9-P2255T diminishes dendritic spine head dimensions

Decreased dendritic spine density on cortical pyramidal neurons is one of the most consistently reported cytological abnormalities in SZ, and patients have also been shown to display altered levels of several regulators of the actin cytoskeleton in spines (39). Therefore, we assessed the density and dimensions of spines in neurons overexpressing Kal9-WT as compared to Kal9-P2255T (Figure 3A). As shown before (10), Kal9-WT significantly increased spine breadth, and also increased spine area, as compared to GFP. Kal9-P2255T reversed this effect, as spine area and breadth were both significantly decreased in neurons transfected with Kal9-P2255T as compared to Kal9-WT, but did not significantly differ from GFP alone (Figure 3B).

Kal9-P2255T protein is expressed at higher levels than Kal9-WT protein levels in neurons

Elevated levels of Kal9 were seen within the auditory cortex of individuals with SZ as compared to psychiatrically normal controls (10), suggesting a potential role in pathogenesis. We therefore tested the impact of the P2255T SNV on Kal9 protein levels in cultured cortical neurons. We co-transfected cells at DIV14 with GFP and either Kal9-WT or Kal9-P2255T, and allowed them to express the exogenous proteins for 72 h. To exclude endogenous Kal9 we labeled the exogenous protein with a c-Myc antibody that only recognizes the exogenous tagged Kal9 (Figure 4A). After 72 h neurons showed a greater amount of Kal9-P2255T compared to Kal9-WT under identical transfection conditions (Figure 4B). To see if this increase in Kal9-P2255T protein was sustained, we allowed neurons to express exogenous proteins for 14 days. We found a similar trend to that seen for 72 h, demonstrating that the increase in Kal9-P2255T is indeed sustained (Figure 4C). Normalization to GFP expression confirmed that the increase in the P2255T at 72 h was not due to differences in transfection efficiency (Figure 4D).

Increased Kal9-P2255T protein is due to altered mRNA stability

To directly test the abundance and biological stability of Kal9-P2255T versus Kal9-WT, we transiently transfected Kal9-WT or Kal9-P2255T-expressing plasmids into hEK293 cells, along with GFP to assess for transfection efficiency. qRT-PCR revealed that Kal9-P2255T mRNA levels were elevated compared to Kal9-WT under the same transfection conditions

(Figure 4E). To test the relative stability of Kal9-WT versus Kal9-P2255T mRNA, after 24 h of overexpression we used actinomycin-D (ActD) to inhibit RNA polymerase and thus any subsequent generation of new transcripts. The half-life curves generated for each transcript show that the single nucleotide difference in the Kal9-P2255T transcript leads to significantly more stable Kal9 mRNA (Figure 4F).

Stability of a specific mRNA molecule is partly determined by its secondary structure. To determine the impact of the P2255T SNV on the Kal9 mRNA (accession AF232668) secondary structure, we used the *mfold* software with default parameters to generate an *in silico* prediction based on free energy minimization using parameters set forth by the nearest-neighbor model (40). The Kal9-P2255T SNV was predicted to diminish the presence of an interior loop structure within a helix (Figure 4G). It should be noted, however, that predicted secondary structure changes may or may not carry over into alterations in biological stability, which is regulated by a combination of sequence-specific RNA-binding proteins, microRNAs (miRNAs), as well as by RNA secondary structure (41–43).

We next sought to determine if the Kal9-P2255T SNV also alters protein stability in hEK293 cells transiently expressing Kal9-WT or Kal9-P2255T, along with GFP to normalize for transfection efficiency. Similar to what was seen in neurons, Kal9-P2255T protein levels were higher than Kal9-WT after 48 h (Figure 4H, I). We then used cycloheximide (CHX) to inhibit new protein synthesis and tested the comparative stability of residual Kal9-WT or Kal9-P2255T proteins. We allowed cells to express exogenous proteins for 24 h, after which we treated cells with cycloheximide and examined Kal9 protein levels at three subsequent time points. The rate of protein degradation did not significantly differ between Kal9-WT and Kal9-P2255T (Figure 4J; Supplemental Figure S2), indicating that the P2255T SNV does not change the stability of Kal9 protein.

The P2255T substitution increases Kal9 RhoA-GEF catalytic activity

The P2255T substitution, while not in the Rho-GEF catalytic domain, occurs only 14 amino acids downstream of it, suggesting that it may affect this activity (Figure 1A: arrow). Upregulation of RhoA activation by overexpression of another RhoA-GEF, ARHGEF11, or constitutively active RhoA, as well as the knockdown of the Rho GTPase activating protein oligophrenin-1, have been shown to reduce dendritic complexity, spine area, and spine density (19–21). We thus sought to determine whether Kal9-P2255T could elicit its effects on neuronal morphology through altered GEF activity. We expressed Kal9-WT and Kal9-P2255T in hEK293 cells and performed a RhoA activation affinity assay to evaluate their impact on GTP-bound RhoA (Figure 5A). To assess intrinsic activity independent on protein levels, we normalized to both total RhoA and exogenous Kal9 levels. Kal9-P2255T expression led to a significant increase in RhoA activation (Figure 5C, upper panel). On the contrary, a similar assay used to measure Rac1 activation did not show any differences in Rac1 activation between Kal9-WT and Kal9-P2255T (Figure 5B, 5C lower panel).

Compound effect of mRNA stability and Rho-GEF activity in Kal9-P2255T

Because the signaling output of a protein is dependent on both intrinsic enzymatic activity and protein levels, we accounted for the differential protein levels between the WT and

P2255T variants. We transfected equal amounts of Kal9-WT and Kal9-P2255T cDNA and when performing RhoA activation assay we normalized to total RhoA (Figure 5D). We found that the RhoA-GEF activity of Kal9-P2255T was enhanced to an even greater degree as compared to Kal9-WT (Figure 5E). Thus, the compound effects of increased RhoA-GEF activity in Kal9-P2255T, with heightened levels carrying this variant, result in a significantly altered signaling output of the protein.

Discussion

Recent discoveries have found that exonic point mutations (SNVs) play an important role in the etiology of mental disorders, including SZ (3, 5, 44). Exome sequencing of large numbers of patients and controls has revealed that small mutations, affecting only a few nucleotides, are overrepresented among glutamatergic postsynaptic proteins, including activity-regulated cytoskeleton-associated proteins, N-methyl-d-aspartate receptor (NMDAR) complexes, and proteins that interact with these complexes to modulate synaptic strength (3, 5). Such mutations are very rare (frequency < 0.5%). None of these SNVs individually were statistically associated with SZ. However, the functional significance of such mutations, especially at sites relevant for these disorders such as dendrites and synapses, has not yet been examined. For these reasons we investigated the impact of a SNV in *KALRN*, enriched in subjects with SZ, on the structure and function of dendrites and synapses in neurons. There currently exist few studies linking rare SZ-associated SNVs to functional deficits. Several SNVs in the *GIT1* gene that were originally identified via exome sequencing of SZ patients were demonstrated to perturb GIT1 protein function with regard to protein-protein interactions and levels of proteins involved in neurotransmission (45).

While the *KALRN* gene locus is not among the 108 well-established GWAS loci (26), it was identified in a smaller GWAS (46). Kushima and colleagues identified several rare missense mutations (SNVs) in the human *KALRN* gene enriched in patients with SZ (6). A global comparison of the frequencies of five selected mutations in *KALRN* between cases and controls showed a significant increase in frequency in SZ patients (OR = 2.07, P = .003). Of these, P2255T showed a significant association with SZ (OR = 2.09, P = .012), and *in silico* analysis via PMut predicted P2255T to be “pathological” (6). Analysis using Polyphen software predicted that the SNV would be “benign”, although this is likely accounted for by differences in the computational methods employed (47). While an OR = 2 may seem small in the context of other genetic mutations, for example CNVs, which have odds ratios that are several times higher, this number is highly significant in context of rare coding point mutations (48). Given that none of the SNVs identified so far in exome sequencing studies (3, 5) show statistical association individually to SZ because they are so rare, *KALRN*-P2255T stands out as one of the strongest associations of a SNV with SZ identified. It is noteworthy that there is a lower than predicted frequency of missense SNVs in the *KALRN* gene in the ExAC database (380 observed versus 617.5 expected; z = 4.67), which suggests that there is a constraint on mutations in the gene and indicates an important biological function for kalirin (49).

Protein and mRNA expression changes and defective kalirin signaling have been consistently reported in studies on postmortem brain tissue of SZ subjects by independent

laboratories. Kalirin mRNA and kalirin-7 protein levels were reduced in the prefrontal cortex of SZ patients, while kalirin-9 was upregulated in the auditory cortex (8–10). Using targeted sequencing, we previously identified a rare coding variant in the *KALRN* gene region that encodes the Rac1-GEF catalytic domain, in a SZ patient and his sibling with major depressive disorder (MDD), which was not present in the control group (35). The D1338N substitution significantly diminished the protein's ability to catalyze Rac1 activation and to increase spine size and density. Remarkably, *KALRN* knockout mice show periadolescent cortical spine loss, deficits in working memory and sensorimotor gating, and other SZ-related phenotypes (50, 51). In spines, kalirin functions downstream of NMDA receptors, neuregulin/ErbB4, 5HT2A receptors, and interacts with DISC1 to control spine remodeling (52). Our bioinformatics analysis further implicates kalirin signaling in molecular pathways relevant for SZ. Kalirin has also been implicated in other neuropsychiatric and neurological disorders such as intellectual disability, Alzheimer's disease, impulsivity, attention-deficit hyperactivity disorder, and ischemic stroke (53–61).

Kal9-P2255T recapitulates some of these key SZ-associated dendritic phenotypes. Reductions in dendritic length, complexity, and spine number in multiple brain regions have been well characterized in SZ (62). Specifically, reduced basilar dendritic length and number have been described in several prefrontal cortical areas, anterior cingulate cortex, and primary visual cortex (28, 63–67). While the P2255T substitution did not alter the effects of Kal9 overexpression on spine density, it did prevent the increase in spine size and breadth caused by expression of Kal9-WT. Changes in the structure of spines as seen following Kal9-WT overexpression are correlated with an increase in the abundance of synaptic AMPA receptors (68). Therefore, Kal9-P2255T may not be able to alter a cell's intrinsic excitability to the extent that Kal9-WT is. With regard to the effects of Kal9-P2255T on basal dendrites, it is notable that the majority of excitatory synapses on layer V cortical pyramidal neurons are located to the basal rather than apical dendrites (69). As such, a reduction in basal dendritic complexity might be expected to give rise to the aberrant cortical circuitry that has been hypothesized to cause certain aspects of SZ psychopathology (70). Impaired signaling to the actin cytoskeleton has also been proposed as an important mechanism in the pathogenesis of schizophrenia, supported by genetic and postmortem findings, as well as *in vivo* models (5, 10, 71, 72). Additionally, beta-tubulin expression and MAP2 immunoreactivity have also been shown to be decreased in schizophrenia (62, 73).

Our functional analysis reveals an unexpected compound effect on mRNA stability and intrinsic RhoA-GEF activity in Kal9-P2255T, unique to our knowledge among disease-associated SNVs. The effect on mRNA stability is particularly interesting. Historically, most attention has been paid to the protein sequence of disease-associated genes. However, single base-pair variations within mRNA can lead to alterations in thermodynamic stability through effects on secondary structure (41). Changes in mRNA stability, folding, and rate of degradation have been shown to be associated with human disease, independent of a change in protein sequence (74).

As a brain-enriched dual Rac1/RhoA-GEF kalirin is in a unique position to regulate dendrite and spine morphology, as both Rac1 and RhoA are involved in dendritic growth and remodeling. Our SIM imaging reveals subcellular distribution differences between kalirin

isoforms that are important for their functions. The Kal9-P2255T SNV may thus change in the balance between RhoA and Rac1 activation, leading to altered dendritic morphology. The combination of increased RhoA activation, as well as elevated Kal9 expression levels, may have a joint effect leading to very high elevation of downstream signaling to the cytoskeleton. Impaired signaling to the actin cytoskeleton has been proposed as an important mechanism in SZ pathogenesis, supported by genetic and postmortem findings, as well as *in vivo* models (5, 10, 71, 72). Investigating the P2255T variant in Kal9, a protein which acts in several pathways involved in cytoskeletal reorganization, could provide a platform for studying pathway perturbations that lead to a SZ-associated neuronal phenotypes.

The current studies were performed in an overexpression system, however, which brings with it the limitations of supraphysiologic expression levels. Future studies should focus on using this mutation in an endogenous setting as a model system to better elucidate potential causes of the altered neuronal morphology characteristic of SZ. Introduction of this SNV at the genetic locus to generate a humanized mouse model would allow for deeper interrogation of SZ-relevant pathway perturbations, as well as direct hypothesis testing of potential pharmacotherapeutic targets within these pathways. Alternatively, induced pluripotent stem cells from Kal-P2255T carriers could be used to generated neurons which would express the variant at endogenous levels. If such neurons displayed morphological deficits compared to those expressing only wildtype kalirin protein, the precise impact of the SNV could be more conclusively determined. Nevertheless, rare mutations can provide powerful tools for modeling disease-associated phenotypes and identifying points of convergence onto common pathways.

Supplementary Material

Refer to Web version on PubMed Central for supplementary material.

Acknowledgments

This work was supported by NIH grants 5R01MH071316-10 (P.P), 3R01MH071533-13S1 (R.A.S), and 5R01MH097216-03 (P.P).

References

1. Rutkowski TP, Schroeder JP, Gafford GM, Warren ST, Weinshenker D, Caspary T, et al. Unraveling the genetic architecture of copy number variants associated with schizophrenia and other neuropsychiatric disorders. Journal of neuroscience research. 2016
2. Gejman PV, Sanders AR, Duan J. The role of genetics in the etiology of schizophrenia. The Psychiatric clinics of North America. 2010; 33:35–66. [PubMed: 20159339]
3. Fromer M, Pocklington AJ, Kavanagh DH, Williams HJ, Dwyer S, Gormley P, et al. De novo mutations in schizophrenia implicate synaptic networks. Nature. 2014; 506:179–184. [PubMed: 24463507]
4. Hall J, Trent S, Thomas KL, O'Donovan MC, Owen MJ. Genetic risk for schizophrenia: convergence on synaptic pathways involved in plasticity. Biol Psychiatry. 2015; 77:52–58. [PubMed: 25152434]
5. Purcell SM, Moran JL, Fromer M, Ruderfer D, Solovieff N, Roussos P, et al. A polygenic burden of rare disruptive mutations in schizophrenia. Nature. 2014; 506:185–190. [PubMed: 24463508]

6. Kushima I, Nakamura Y, Aleksic B, Ikeda M, Ito Y, Shiino T, et al. Resequencing and association analysis of the KALRN and EPHB1 genes and their contribution to schizophrenia susceptibility. Schizophr Bull. 2012; 38:552–560. [PubMed: 21041834]
7. Sullivan PF, Daly MJ, O'Donovan M. Genetic architectures of psychiatric disorders: the emerging picture and its implications. Nat Rev Genet. 2012; 13:537–551. [PubMed: 22777127]
8. Hill JJ, Hashimoto T, Lewis DA. Molecular mechanisms contributing to dendritic spine alterations in the prefrontal cortex of subjects with schizophrenia. Mol Psychiatry. 2006; 11:557–566. [PubMed: 16402129]
9. Rubio MD, Haroutunian V, Meador-Woodruff JH. Abnormalities of the Duo/Ras-related C3 botulinum toxin substrate 1/p21-activated kinase 1 pathway drive myosin light chain phosphorylation in frontal cortex in schizophrenia. Biological Psychiatry. 2012; 71:906–914. [PubMed: 22458949]
10. Deo AJ, Cahill ME, Li S, Goldszer I, Henteleff R, Vanleeuwen JE, et al. Increased expression of Kalirin-9 in the auditory cortex of schizophrenia subjects: its role in dendritic pathology. Neurobiol Dis. 2012; 45:796–803. [PubMed: 22120753]
11. Penzes P, Johnson RC, Kambampati V, Mains RE, Eipper BA. Distinct roles for the two Rho GDP/GTP exchange factor domains of kalirin in regulation of neurite growth and neuronal morphology. J Neurosci. 2001; 21:8426–8434. [PubMed: 11606631]
12. Johnson RC, Penzes P, Eipper BA, Mains RE. Isoforms of kalirin, a neuronal Dbl family member, generated through use of different 5'- and 3'-ends along with an internal translational initiation site. J Biol Chem. 2000; 275:19324–19333. [PubMed: 10777487]
13. Tolias KF, Duman JG, Um K. Control of synapse development and plasticity by Rho GTPase regulatory proteins. Prog Neurobiol. 2011; 94:133–148. [PubMed: 21530608]
14. Duman JG, Mulherkar S, Tu YK, J XC, Tolias KF. Mechanisms for spatiotemporal regulation of Rho-GTPase signaling at synapses. Neurosci Lett. 2015; 601:4–10. [PubMed: 26003445]
15. Soderling SH, Guire ES, Kaech S, White J, Zhang F, Schutz K, et al. A WAVE-1 and WRP signaling complex regulates spine density, synaptic plasticity, and memory. J Neurosci. 2007; 27:355–365. [PubMed: 17215396]
16. Wegner AM, Nebhan CA, Hu L, Majumdar D, Meier KM, Weaver AM, et al. N-wasp and the arp2/3 complex are critical regulators of actin in the development of dendritic spines and synapses. J Biol Chem. 2008; 283:15912–15920. [PubMed: 18430734]
17. Meng Y, Zhang Y, Tregoubov V, Janus C, Cruz L, Jackson M, et al. Abnormal spine morphology and enhanced LTP in LIMK-1 knockout mice. Neuron. 2002; 35:121–133. [PubMed: 12123613]
18. Hedrick NG, Harward SC, Hall CE, Murakoshi H, McNamara JO, Yasuda R. Rho GTPase complementation underlies BDNF-dependent homo- and heterosynaptic plasticity. Nature. 2016; 538:104–108. [PubMed: 27680697]
19. Govek EE, Newey SE, Akerman CJ, Cross JR, Van der Veken L, Van Aelst L. The X-linked mental retardation protein oligophrenin-1 is required for dendritic spine morphogenesis. Nat Neurosci. 2004; 7:364–372. [PubMed: 15034583]
20. Mizuki Y, Takaki M, Sakamoto S, Okamoto S, Kishimoto M, Okahisa Y, et al. Human Rho Guanine Nucleotide Exchange Factor 11 (ARHGEF11) Regulates Dendritic Morphogenesis. International journal of molecular sciences. 2016; 18
21. Nakayama AY, Harms MB, Luo L. Small GTPases Rac and Rho in the maintenance of dendritic spines and branches in hippocampal pyramidal neurons. J Neurosci. 2000; 20:5329–5338. [PubMed: 10884317]
22. Hayashi-Takagi A, Takaki M, Graziane N, Seshadri S, Murdoch H, Dunlop AJ, et al. Disrupted-in-Schizophrenia 1 (DISC1) regulates spines of the glutamate synapse via Rac1. Nat Neurosci. 2010; 13:327–332. [PubMed: 20139976]
23. Cahill ME, Remmers C, Jones KA, Xie Z, Sweet RA, Penzes P. Neuregulin1 signaling promotes dendritic spine growth through kalirin. Journal of neurochemistry. 2013; 126:625–635. [PubMed: 23742124]
24. Morrow EM, Kane A, Goff DC, Walsh CA. Sequence analysis of P21-activated kinase 3 (PAK3) in chronic schizophrenia with cognitive impairment. Schizophr Res. 2008; 106:265–267. [PubMed: 18805672]

25. Mulle JG, Dodd AF, McGrath JA, Wolyniec PS, Mitchell AA, Shetty AC, et al. Microdeletions of 3q29 confer high risk for schizophrenia. Am J Hum Genet. 2010; 87:229–236. [PubMed: 20691406]
26. Consortium SWGotPG. Biological insights from 108 schizophrenia-associated genetic loci. Nature. 2014; 511:421–427. [PubMed: 25056061]
27. Warde-Farley D, Donaldson SL, Comes O, Zuberi K, Badrawi R, Chao P, et al. The GeneMANIA prediction server: biological network integration for gene prioritization and predicting gene function. Nucleic Acids Res. 2010; 38:W214–220. [PubMed: 20576703]
28. Glantz LA, Lewis DA. Decreased dendritic spine density on prefrontal cortical pyramidal neurons in schizophrenia. Arch Gen Psychiatry. 2000; 57:65–73. [PubMed: 10632234]
29. Sweet RA, Henteleff RA, Zhang W, Sampson AR, Lewis DA. Reduced dendritic spine density in auditory cortex of subjects with schizophrenia. Neuropsychopharmacology. 2009; 34:374–389. [PubMed: 18463626]
30. Wills ZP, Mandel-Brehm C, Mardinly AR, McCord AE, Giger RJ, Greenberg ME. The nogo receptor family restricts synapse number in the developing hippocampus. Neuron. 2012; 73:466–481. [PubMed: 22325200]
31. Xia Z, Dudek H, Miranti CK, Greenberg ME. Calcium influx via the NMDA receptor induces immediate early gene transcription by a MAP kinase/ERK-dependent mechanism. J Neurosci. 1996; 16:5425–5436. [PubMed: 8757255]
32. Schindelin J, Arganda-Carreras I, Frise E, Kaynig V, Longair M, Pietzsch T, et al. Fiji: an open-source platform for biological-image analysis. Nature methods. 2012; 9:676–682. [PubMed: 22743772]
33. Woolfrey KM, Srivastava DP, Photowala H, Yamashita M, Barbolina MV, Cahill ME, et al. Epac2 induces synapse remodeling and depression and its disease-associated forms alter spines. Nat Neurosci. 2009; 12:1275–1284. [PubMed: 19734897]
34. Smith KR, Kopeikina KJ, Fawcett-Patel JM, Leaderbrand K, Gao R, Schurmann B, et al. Psychiatric risk factor ANK3/ankyrin-G nanodomains regulate the structure and function of glutamatergic synapses. Neuron. 2014; 84:399–415. [PubMed: 25374361]
35. Russell TA, Blizinsky KD, Cobia DJ, Cahill ME, Xie Z, Sweet RA, et al. A sequence variant in human KALRN impairs protein function and coincides with reduced cortical thickness. Nature communications. 2014; 5:4858.
36. Gustafsson MG. Nonlinear structured-illumination microscopy: wide-field fluorescence imaging with theoretically unlimited resolution. Proc Natl Acad Sci U S A. 2005; 102:13081–13086. [PubMed: 16141335]
37. Branco T, Hausser M. Synaptic integration gradients in single cortical pyramidal cell dendrites. Neuron. 2011; 69:885–892. [PubMed: 21382549]
38. Gordon U, Polsky A, Schiller J. Plasticity compartments in basal dendrites of neocortical pyramidal neurons. J Neurosci. 2006; 26:12717–12726. [PubMed: 17151275]
39. Yan Z, Kim E, Datta D, Lewis DA, Soderling SH. Synaptic Actin Dysregulation, a Convergent Mechanism of Mental Disorders? J Neurosci. 2016; 36:11411–11417. [PubMed: 27911743]
40. Zuker M. Mfold web server for nucleic acid folding and hybridization prediction. Nucleic Acids Res. 2003; 31:3406–3415. [PubMed: 12824337]
41. Chamary JV, Hurst LD. Evidence for selection on synonymous mutations affecting stability of mRNA secondary structure in mammals. Genome biology. 2005; 6:R75. [PubMed: 16168082]
42. Duan J, Wainwright MS, Comeron JM, Saitou N, Sanders AR, Gelernter J, et al. Synonymous mutations in the human dopamine receptor D2 (DRD2) affect mRNA stability and synthesis of the receptor. Hum Mol Genet. 2003; 12:205–216. [PubMed: 12554675]
43. Lennox AL, Mao H, Silver DL. RNA on the brain: emerging layers of post-transcriptional regulation in cerebral cortex development. Wiley interdisciplinary reviews Developmental biology. 2017
44. Iossifov I, O'Roak BJ, Sanders SJ, Ronemus M, Krumm N, Levy D, et al. The contribution of de novo coding mutations to autism spectrum disorder. Nature. 2014; 515:216–221. [PubMed: 25363768]

45. Kim MJ, Biag J, Fass DM, Lewis MC, Zhang Q, Fleishman M, et al. Functional analysis of rare variants found in schizophrenia implicates a critical role for GIT1-PAK3 signaling in neuroplasticity. Mol Psychiatry. 2016
46. Ikeda M, Aleksic B, Kinoshita Y, Okochi T, Kawashima K, Kushima I, et al. Genome-wide association study of schizophrenia in a Japanese population. Biol Psychiatry. 2011; 69:472–478. [PubMed: 20832056]
47. Wei Q, Wang L, Wang Q, Kruger WD, Dunbrack RL Jr. Testing computational prediction of missense mutation phenotypes: functional characterization of 204 mutations of human cystathionine beta synthase. Proteins. 2010; 78:2058–2074. [PubMed: 20455263]
48. Harrison PJ. The current and potential impact of genetics and genomics on neuropsychopharmacology. European neuropsychopharmacology : the journal of the European College of Neuropsychopharmacology. 2015; 25:671–681. [PubMed: 23528807]
49. Lek M, Karczewski KJ, Minikel EV, Samocha KE, Banks E, Fennell T, et al. Analysis of protein-coding genetic variation in 60,706 humans. Nature. 2016; 536:285–291. [PubMed: 27535533]
50. Cahill ME, Xie Z, Day M, Photowala H, Barbolina MV, Miller CA, et al. Kalirin regulates cortical spine morphogenesis and disease-related behavioral phenotypes. Proc Natl Acad Sci U S A. 2009; 106:13058–13063. [PubMed: 19625617]
51. Xie Z, Cahill ME, Penzes P. Kalirin loss results in cortical morphological alterations. Mol Cell Neurosci. 2010; 43:81–89. [PubMed: 19800004]
52. Penzes P, Remmers C. Kalirin signaling: implications for synaptic pathology. Molecular Neurobiology. 2012; 45:109–118. [PubMed: 22194219]
53. Dang M, Wang Z, Zhang R, Li X, Peng Y, Han X, et al. KALRN Rare and Common Variants and Susceptibility to Ischemic Stroke in Chinese Han Population. Neuromolecular medicine. 2015; 17:241–250. [PubMed: 25917671]
54. Cai DC, Fonteijn H, Guadalupe T, Zwiers M, Wittfeld K, Teumer A, et al. A genome-wide search for quantitative trait loci affecting the cortical surface area and thickness of Heschl's gyrus. Genes Brain Behav. 2014; 13:675–685. [PubMed: 25130324]
55. Makrythanasis P, Guipponi M, Santoni FA, Zaki M, Issa MY, Ansar M, et al. Exome sequencing discloses KALRN homozygous variant as likely cause of intellectual disability and short stature in a consanguineous pedigree. Human genomics. 2016; 10:26. [PubMed: 27421267]
56. Ward-Caviness C, Haynes C, Blach C, Dowdy E, Gregory SG, Shah SH, et al. Gene-smoking interactions in multiple Rho-GTPase pathway genes in an early-onset coronary artery disease cohort. Hum Genet. 2013; 132:1371–1382. [PubMed: 23907653]
57. DeWan AT, Egan KB, Hellenbrand K, Sorrentino K, Pizzoferrato N, Walsh KM, et al. Whole-exome sequencing of a pedigree segregating asthma. BMC medical genetics. 2012; 13:95. [PubMed: 23046476]
58. Krug T, Manso H, Gouveia L, Sobral J, Xavier JM, Albergaria I, et al. Kalirin: a novel genetic risk factor for ischemic stroke. Hum Genet. 2010; 127:513–523. [PubMed: 20107840]
59. Horne BD, Hauser ER, Wang L, Muhlestein JB, Anderson JL, Carlquist JF, et al. Validation study of genetic associations with coronary artery disease on chromosome 3q13–21 and potential effect modification by smoking. Annals of human genetics. 2009; 73:551–558. [PubMed: 19706030]
60. Lesch KP, Timmesfeld N, Renner TJ, Halperin R, Roser C, Nguyen TT, et al. Molecular genetics of adult ADHD: converging evidence from genome-wide association and extended pedigree linkage studies. J Neural Transm (Vienna). 2008; 115:1573–1585. [PubMed: 18839057]
61. Wang L, Hauser ER, Shah SH, Pericak-Vance MA, Haynes C, Crosslin D, et al. Peakwide mapping on chromosome 3q13 identifies the kalirin gene as a novel candidate gene for coronary artery disease. Am J Hum Genet. 2007; 80:650–663. [PubMed: 17357071]
62. Moyer CE, Shelton MA, Sweet RA. Dendritic spine alterations in schizophrenia. Neurosci Lett. 2015; 601:46–53. [PubMed: 25478958]
63. Black JE, Kodish IM, Grossman AW, Klintsova AY, Orlovskaya D, Vostrikov V, et al. Pathology of layer V pyramidal neurons in the prefrontal cortex of patients with schizophrenia. Am J Psychiatry. 2004; 161:742–744. [PubMed: 15056523]
64. Broadbelt K, Byne W, Jones LB. Evidence for a decrease in basilar dendrites of pyramidal cells in schizophrenic medial prefrontal cortex. Schizophr Res. 2002; 58:75–81. [PubMed: 12363393]

65. Kalus P, Muller TJ, Zuschratter W, Senitz D. The dendritic architecture of prefrontal pyramidal neurons in schizophrenic patients. Neuroreport. 2000; 11:3621–3625. [PubMed: 11095531]

66. Kolluri N, Sun Z, Sampson AR, Lewis DA. Lamina-specific reductions in dendritic spine density in the prefrontal cortex of subjects with schizophrenia. Am J Psychiatry. 2005; 162:1200–1202. [PubMed: 15930070]

67. Konopaske GT, Lange N, Coyle JT, Benes FM. Prefrontal cortical dendritic spine pathology in schizophrenia and bipolar disorder. JAMA psychiatry. 2014; 71:1323–1331. [PubMed: 25271938]

68. Fu AK, Ip NY. Regulation of postsynaptic signaling in structural synaptic plasticity. Current opinion in neurobiology. 2017; 45:148–155. [PubMed: 28600964]

69. Larkman AU. Dendritic morphology of pyramidal neurones of the visual cortex of the rat: III. Spine distributions. J Comp Neurol. 1991; 306:332–343. [PubMed: 1711059]

70. Lisman JE, Coyle JT, Green RW, Javitt DC, Benes FM, Heckers S, et al. Circuit-based framework for understanding neurotransmitter and risk gene interactions in schizophrenia. Trends Neurosci. 2008; 31:234–242. [PubMed: 18395805]

71. Datta D, Arion D, Corradi JP, Lewis DA. Altered expression of CDC42 signaling pathway components in cortical layer 3 pyramidal cells in schizophrenia. Biol Psychiatry. 2015; 78:775–785. [PubMed: 25981171]

72. Kim IH, Racz B, Wang H, Burianek L, Weinberg R, Yasuda R, et al. Disruption of Arp2/3 results in asymmetric structural plasticity of dendritic spines and progressive synaptic and behavioral abnormalities. J Neurosci. 2013; 33:6081–6092. [PubMed: 23554489]

73. English JA, Dicker P, Focking M, Dunn MJ, Cotter DR. 2-D DIGE analysis implicates cytoskeletal abnormalities in psychiatric disease. Proteomics. 2009; 9:3368–3382. [PubMed: 19562803]

74. Gotea V, Gartner JJ, Qutob N, Elnitski L, Samuels Y. The functional relevance of somatic synonymous mutations in melanoma and other cancers. Pigment Cell Melanoma Res. 2015; 28:673–684. [PubMed: 26300548]

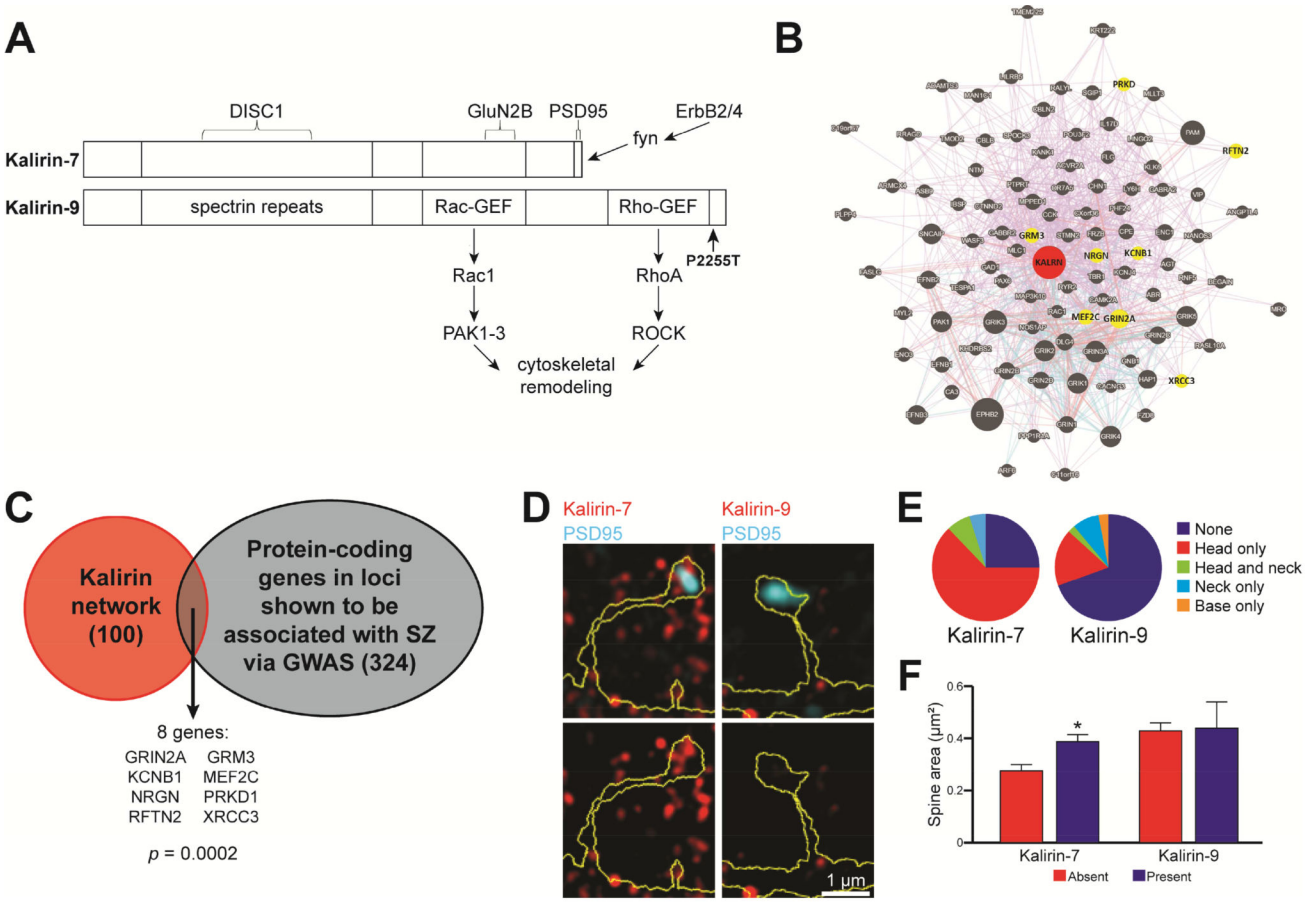

Figure 1.

KALRN associations with SZ and expression in mature neurons. A. Schematic of the Kal7 and Kal9 proteins, showing catalytic domains, structural motifs, and upstream and downstream signaling pathways. The location of the P2255T substitution in Kal9 is indicated by an arrow. Asterisk indicates the PDZ-binding domain specific to Kal7. The location of the P2255T substitution is shown. B. Hypothetical *KALRN* interaction network, predicted based on co-expression, pathway, and physical interaction, and weighted with regard to cellular component gene ontology. Genes shown in yellow are also among those residing in SZ-associated loci identified by a large-scale GWAS. A high-resolution rendering of this network is included in Supplemental Figure S1. C. Hypergeometric testing reveals a significant overlap between those genes in the hypothetical *KALRN* network and those identified by GWAS. D. SIM imaging of mature (DIV 25–26) cortical neurons demonstrates that endogenous kalirin-7 is localized in the majority of PSD95-containing spines, whereas kalirin-9 is largely excluded from spines. E. Proportions of spines with Kal7 and Kal9 expression in distinct nanodomains. Blue: no expression; red: head only; green: head and neck; purple: head and base: light blue: neck only; orange: base only. F. Spines lacking kalirin-7 are significantly smaller than those with kalirin-7 (N=98 spines). The presence of kalirin-9 in a spine has no bearing on its size (N=113 spines). Cells from three independent experiments were analyzed. Data are mean ± SEM. *, $p<0.05$.

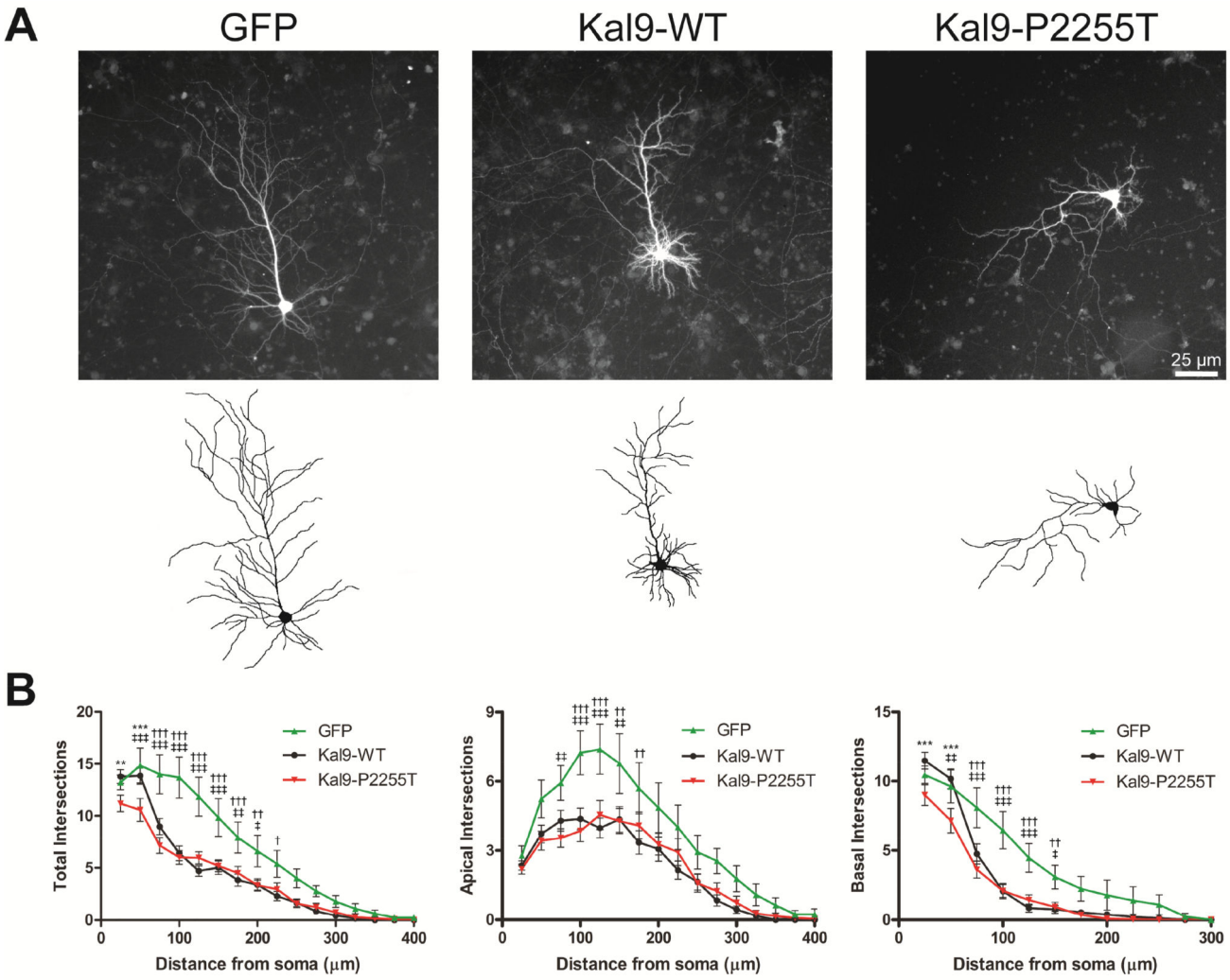

Figure 2.

Kal9-P2255T diminishes basal dendrite branching in cortical pyramidal neurons. A. DIV25–26 neurons transfected with either GFP alone, or with GFP and either Kal9-WT or Kal9-P2255T (upper panels); and traces used for Sholl analysis (lower panels). B. Sholl analysis reveals a significant reduction in basal dendrites of neurons expressing Kal9-P2255T extending 25 and 50 µm from the soma as compared to Kal9-WT. Apical dendrites were unchanged. N=20–35 neurons per transfection condition from three independent experiments. Data are mean ± SEM. **, $p<0.01$; ***, $p<0.005$ (Kal9-WT vs. Kal9-P2255T). †, $p<0.05$; ††, $p<0.01$; †††, $p<0.005$ (Kal9-WT vs. GFP). ‡, $p<0.05$; ‡‡, $p<0.01$; ‡‡‡, $p<0.005$ (Kal9-P2255T vs. GFP).

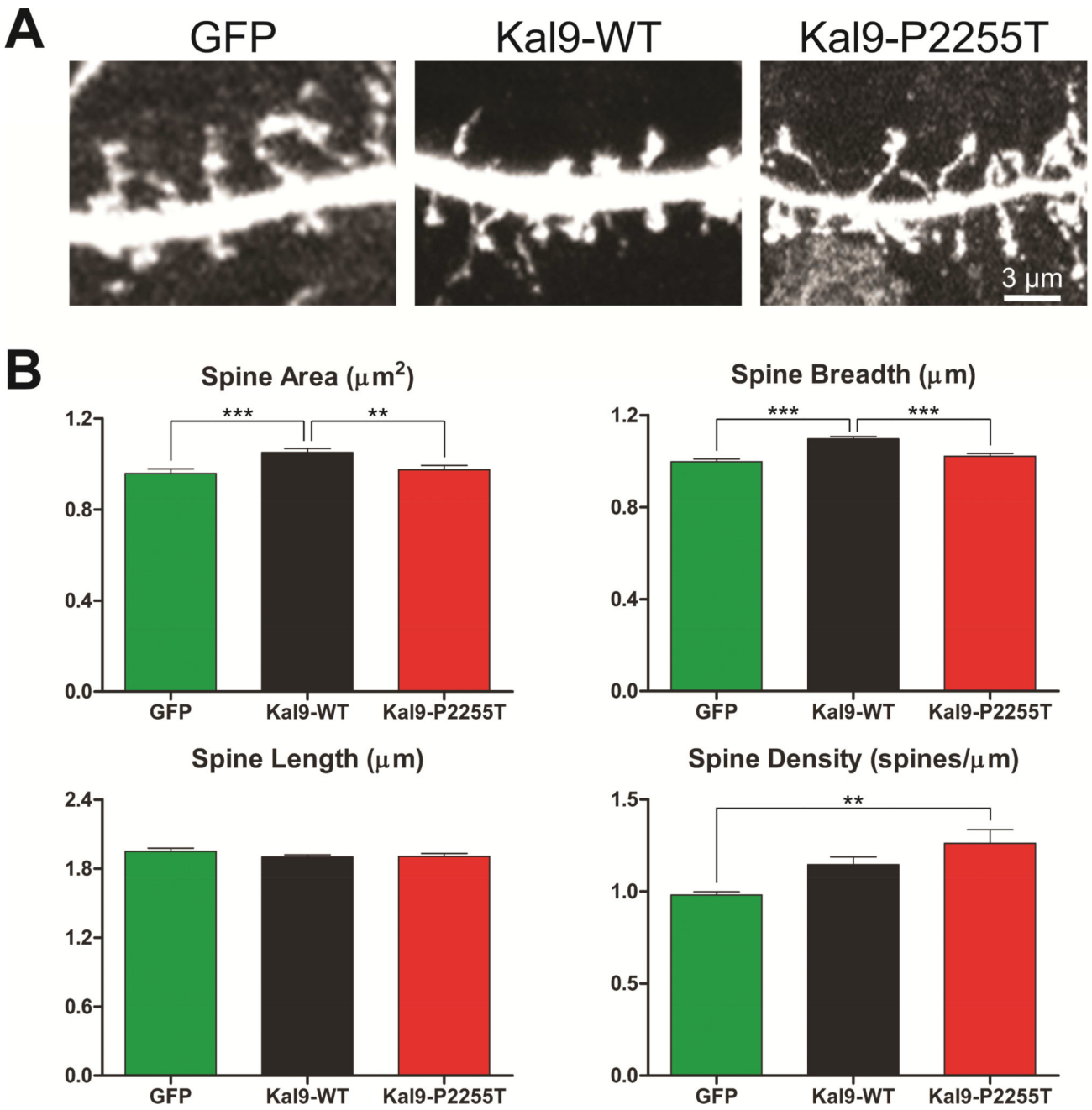

Figure 3.

Kal9-P2255T fails to induce the increases in dendritic spine dimensions seen following Kal9-WT overexpression. A. DIV25–26 cortical pyramidal neurons transfected with either GFP alone, or with GFP and either Kal9-WT or Kal9-P2255T. B. Area and breadth of dendritic spine heads are significantly reduced in neurons expressing Kal9-P2255T as compared to Kal9-WT. Spine length and density were unaffected. 11–18 neurons per transfection condition from three independent experiments were analyzed. Data are mean ± SEM. **, $p<0.01$; ***, $p<0.005$.

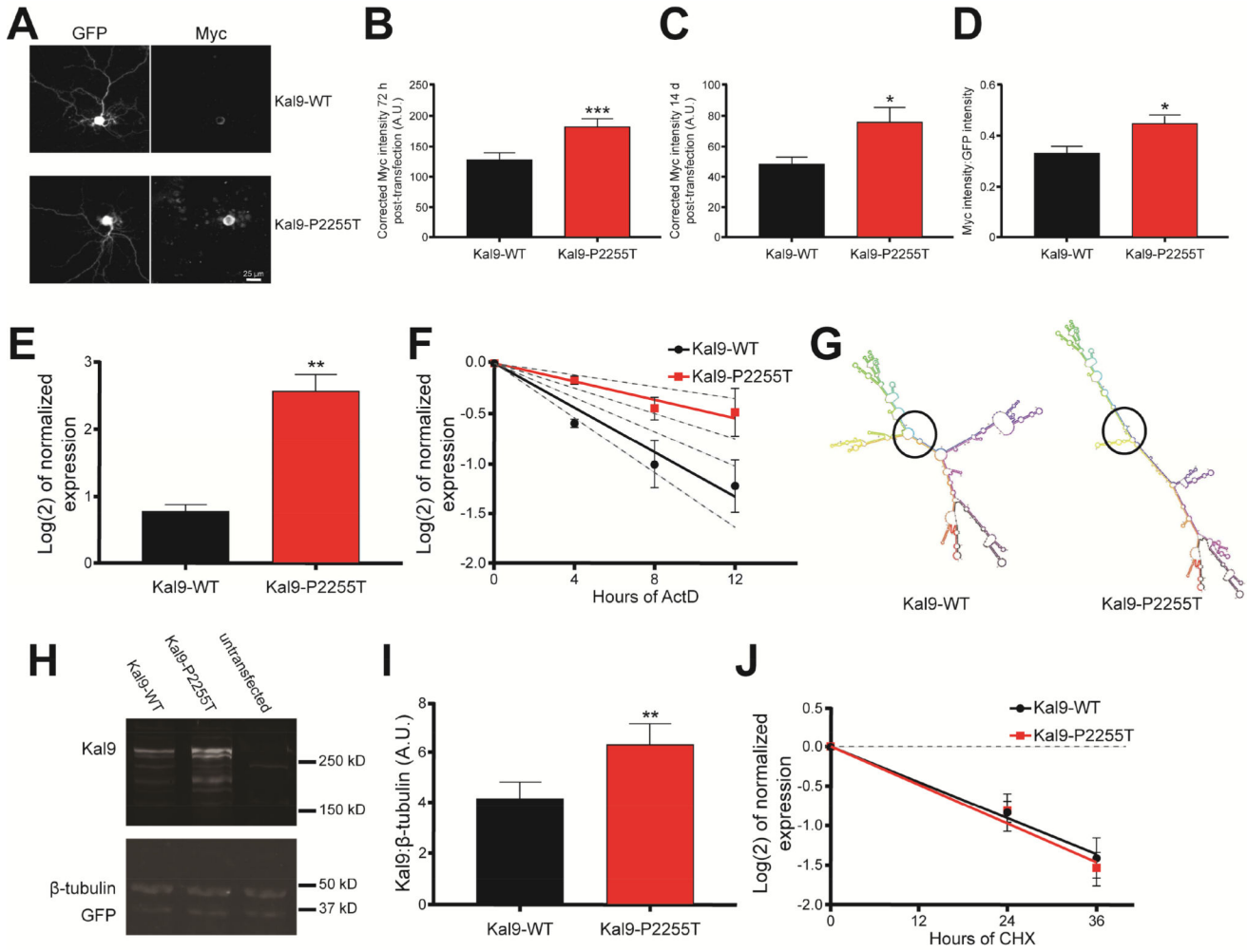

Figure 4.

Kal9-P2255T protein and mRNA are expressed more highly than Kal9-WT. A. DIV 28 cortical pyramidal neurons transfected with GFP and either Kal9-WT or Kal9-P2255T and stained for GFP and c-Myc. B, C. Fluorescence intensity of Kal9-P2255T is greater than that of Kal9-WT at both 72 h (B) and 14 d (C) post-transfection. D. The ratio of c-Myc to GFP intensity reveals that the difference in expression at 72 h is not due to a difference in transfection efficiency. N=68–131 neurons per transfection condition from three independent experiments. E. Isolated RNA from hEK293 cells transfected with either Kal9-WT or Kal9-P2255T was subjected to qRT-PCR. Following normalization to β-actin expression, Kal9-P2255T mRNA levels are shown to be increased compared to Kal9-WT. Data are from four independent experiments. F. Kal9-WT and Kal9-P2255T transfected hEK293 cells treated with ActD for 4, 8, or 12 hours show differential rates of Kal9 transcript degradation. Half-life was calculated as ln(2)/-slope. $t_{1/2}$ = 6.2 hours for Kal9-WT and 15.3 hours for Kal9-P2255T. Dashed lines represent 95% confidence intervals. Data are from three independent experiments. G. *mfold* software predicts the disruption of an interior loop in the secondary structure of Kal9-P2255T mRNA. The nucleotide coding for amino acid 2255 resides in within the circles overlaying the images. H. Western blots of lysates from hEK293 cells

transfected with GFP alone, or GFP and either Kal9-WT or Kal9-P2255T. I. When normalized to β-tubulin, Kal9-P2255T is shown to be expressed more highly than Kal9-WT. J. CHX treatment of transfected hEK293 cells demonstrates that there is no change in the stability of Kal9-P2255T versus Kal9-WT protein (see Supplemental Figure S2 for blot images). Data are from three independent experiments. All data are mean ± SEM. *, $p<0.05$; **, $p<0.01$; ***, $p<0.005$.

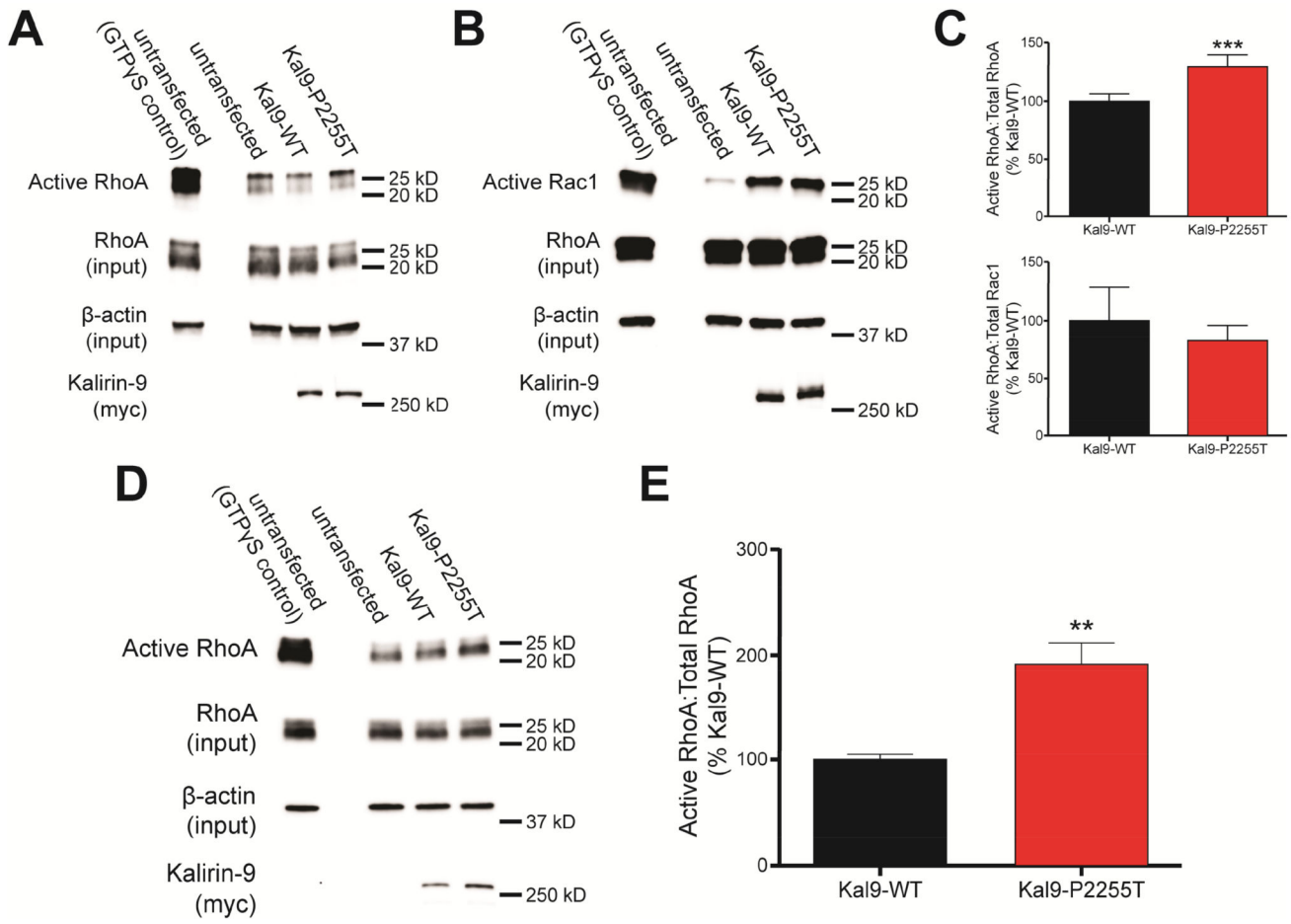

Figure 5.

The P2255T substitution increases Kal9 RhoA-GEF catalytic activity. A. Following transfection of hEK293 cells with amounts of plasmid to account for altered Kal9 protein levels, Western blotting reveals that Kal9-P2255T-transfected cells display higher levels of GTP-bound RhoA than Kal9-WT-transfected cells. B. Under the same transfection conditions as in A, GTP-bound Rac1 levels show no difference between the Kal9-WT and Kal9-P2255T. C. Quantification of the blots in A (upper panel) and B (lower panel). Blots were normalized to total RhoA or Rac1 levels, and β-actin levels. Data are from 4–5 independent experiments. D, E. When equal amounts of Kal9-WT and Kal9-P2255T plasmids are used for transfection, an even greater level of RhoA activation is seen in the Kal9-P2255T condition than that in the experiments described in A. Data are from three independent experiments. All data are mean ± SEM. **, $p<0.01$; ***, $p<0.005$.